

**CENTRAL PRODUCTION OF GLUONIC AND QUARK-ANTIQUARK
DIJETS AND BACKGROUND TO CENTRAL PRODUCTION OF
HIGGS BOSON ***

A. SZCZUREK

Rzeszów University, Rzeszów, Poland and
Institute of Nuclear Physics, Kraków, Poland
E-mail: antoni.szczurek@ifj.edu.pl

We discuss exclusive central production of Higgs boson, quark-antiquark and digluon dijets. Several differential distributions are shown and discussed. Irreducible leading-order $b\bar{b}$ background to Higgs production is calculated in several kinematical variables. The signal-to-background ratio is shown and several improvements are suggested by imposing cuts on b (\bar{b}) transverse momenta and rapidities.

1 Introduction

Some time ago Khoze, Martin and Ryskin developed a QCD approach for exclusive production of Higgs boson [1]. The approach can be easily generalized to other exclusive processes. Recently we have applied this approach to Standard Model Higgs boson, quark-antiquark and digluon exclusive production [2, 3, 4, 5].

Since the cross section for exclusive Higgs boson production is rather small, only $b\bar{b}$ final state can be used to identify Higgs boson. This means that a $b\bar{b}$ continuum background is of crucial importance. Here we discuss this irreducible background.

In our calculations we include exact matrix elements and perform full three- or four-body calculations for all considered processes. The kinematically complete calculations allow to include cuts on kinematical variables which is very useful in order to identify the Higgs boson signal.

*This work was partially supported by the polish grant MNiSW N N20224900235.

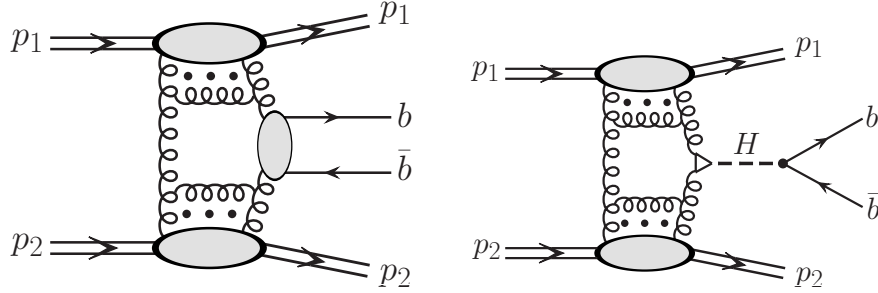


Figure 1: The diagrams for the Higgs and background production.

2 Formalism

Let us concentrate on the simplest case of the production of $q\bar{q}$ pair in the color singlet state (see Fig.1). Color octet state would demand an emission of an extra gluon which considerably complicates the calculations. We do not consider the $q\bar{q}g$ contribution as it is higher order compared to the one considered here.

We write here only the amplitude of the exclusive diffractive $q\bar{q}$ pair production $pp \rightarrow p(q\bar{q})p$ in the color singlet state as ¹

$$\mathcal{M}_{\lambda_q \lambda_{\bar{q}}}^{pp \rightarrow pp q\bar{q}}(p'_1, p'_2, k_1, k_2) = s \cdot \pi^2 \frac{1}{2} \frac{\delta_{c_1 c_2}}{N_c^2 - 1} \Im \int d^2 q_{0,t} V_{\lambda_q \lambda_{\bar{q}}}^{c_1 c_2}(q_1, q_2, k_1, k_2) \frac{f_{g,1}^{\text{off}}(x_1, x'_1, q_{0,t}^2, q_{1,t}^2, t_1) f_{g,2}^{\text{off}}(x_2, x'_2, q_{0,t}^2, q_{2,t}^2, t_2)}{q_{0,t}^2 q_{1,t}^2 q_{2,t}^2}, \quad (1)$$

where $\lambda_q, \lambda_{\bar{q}}$ are helicities of heavy q and \bar{q} , respectively. Above f_1^{off} and f_2^{off} are the off-diagonal unintegrated gluon distributions in nucleon 1 and 2, respectively. The longitudinal momentum fractions of active gluons are calculated based on kinematical variables of outgoing quark and antiquark. The bare amplitude above is subjected to absorption corrections. The absorption corrections are taken here in a multiplicative form.

The color singlet $q\bar{q}$ pair production amplitude can be written as [4]

$$V_{\lambda_q \lambda_{\bar{q}}}^{c_1 c_2}(q_1, q_2, k_1, k_2) \equiv n_\mu^+ n_\nu^- V_{\lambda_q \lambda_{\bar{q}}}^{c_1 c_2, \mu\nu}(q_1, q_2, k_1, k_2),$$

The tensorial part of the amplitude is obtained from Feynman diagrams:

$$V_{\lambda_q \lambda_{\bar{q}}}^{\mu\nu}(q_1, q_2, k_1, k_2) = g_s^2 \bar{u}_{\lambda_q}(k_1) \left(\gamma^\nu \frac{\hat{q}_1 - \hat{k}_1 - m}{(q_1 - k_1)^2 - m^2} \gamma^\mu - \gamma^\mu \frac{\hat{q}_1 - \hat{k}_2 + m}{(q_1 - k_2)^2 - m^2} \gamma^\nu \right) v_{\lambda_{\bar{q}}}(k_2). \quad (2)$$

¹It is straightforward to write the amplitude for the other processes considered here.

The coupling constants $g_s^2 \rightarrow g_s(\mu_{r,1}^2)g_s(\mu_{r,2}^2)$. In the present calculation we take the renormalization scale to be $\mu_{r,1}^2 = \mu_{r,2}^2 = M_{q\bar{q}}^2$. The exact matrix element is calculated numerically. Analytical formulae are shown explicitly in [4].

The off-diagonal parton distributions (i=1,2) are calculated as

$$f_i^{\text{KMR}}(x_i, Q_{i,t}^2, \mu_i^2, t_i) = R_g \frac{d[g(x_i, k_i^2)S_{1/2}(k_i^2, \mu_i^2)]}{d \log k_i^2} \Big|_{k_i^2=Q_{i,t}^2} F(t_i), \quad (3)$$

where $S_{1/2}(q_t^2, \mu^2)$ is a Sudakov-like form factor relevant for the case under consideration. It is reasonable to take the factorization scale as: $\mu_1^2 = \mu_2^2 = M_{q\bar{q}}^2$.

The factor R_g here cannot be calculated from first principles in the most general case of off-diagonal UGDFs. It can be estimated in the case of off-diagonal collinear PDFs when $x' \ll x$ and $xg = x^{-\lambda}(1-x)^n$. Typically $R_g \sim 1.3 - 1.4$ at the Tevatron energy. The off-diagonal form factors are parametrized here as $F(t) = \exp(B_{\text{off}}t)$. In practical calculations we take $B_{\text{off}} = 2 \text{ GeV}^{-2}$. In evaluating f_1 and f_2 needed for calculating the amplitude (1) we use different collinear distributions.

3 Results

In our published papers [3, 4] we have calculated differential cross sections not only for exclusive Higgs boson production but also for $b\bar{b}$ and digluon gg production. In all our calculations we take into account off-shellness of the gluons initiating a relevant hard subprocess. The details about the off-shell matrix element for Higgs boson production can be found in Ref. [7]. In contrast to the exclusive production of χ_c mesons [6], here due to a large factorization scale $\sim M_H$, the off-shell effects for $g^*g^* \rightarrow H$ give only a few percent change of the cross section compared to the calculation with on-shell matrix elements used in the literature. We use the same unintegrated gluon distributions for Higgs, continuum $b\bar{b}$ and digluon production.

The Higgs boson differential cross sections are calculated assuming a three-body process $pp \rightarrow pHp$. Assuming full coverage for outgoing protons we construct two-dimensional distributions $d\sigma/dy d^2p_t$ in Higgs rapidity and transverse momentum. The distribution is used then in a simple Monte Carlo code which includes the Higgs boson decay into the $b\bar{b}$ channel. It is checked subsequently whether b and \bar{b} enter into the region spanned by the central detector.

In the left panel of Fig.2 we show the double diffractive contribution for the CTEQ6 [8] collinear gluon distribution and the contribution from the decay of the Higgs boson including decay width calculated as in Ref. [9], see the sharp peak at $M_{b\bar{b}} = 120 \text{ GeV}$.

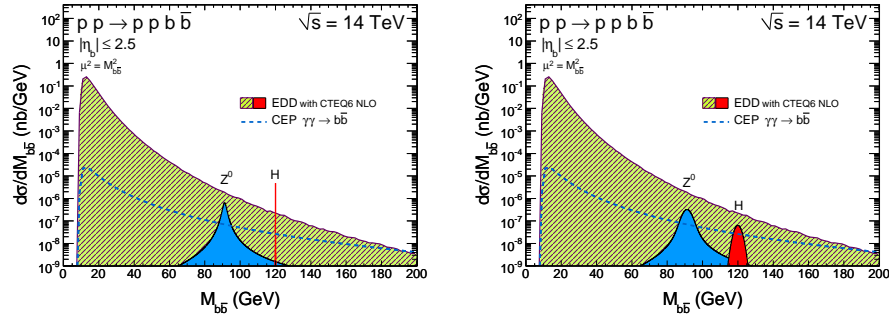


Figure 2: The $b\bar{b}$ invariant mass distribution for $\sqrt{s} = 14$ TeV and for b and \bar{b} jets for $-2.5 < \eta < 2.5$ corresponding to the ATLAS and CMS detectors. The left panel shows purely theoretical predictions, while the right panel includes experimental effects due to experimental uncertainty in missing mass measurement.

The phase space integrated cross section for the Higgs production, including absorption effects with gap survival probability $S_G = 0.03$ is less than 1 fb. The result shown in Fig.2 includes branching fraction for $BR(H \rightarrow b\bar{b}) \approx 0.8$ and the rapidity restrictions. The much broader Breit-Wigner type peak to the left of the Higgs signal corresponds to the exclusive production of the Z^0 boson with the cross section calculated as in Ref. [10]. The branching fraction $BR(Z^0 \rightarrow b\bar{b}) \approx 0.15$ has been included in addition. In contrast to the Higgs case the absorption effects for the Z^0 production are much smaller [10]. The sharp peak corresponding to the Higgs boson clearly sticks above the background.

In reality the situation is much worse as both protons and b and \bar{b} jets are measured with a certain precision which automatically leads to a smearing in $M_{b\bar{b}}$. Experimentally instead of $M_{b\bar{b}}$ one will measure rather two-proton missing mass. In our calculations the experimental effects are included in the simplest way by a convolution of the theoretical distributions with the Gaussian smearing function with $\sigma = 2$ GeV which is due to the precision of measuring forward protons. In the right panel we show the two-proton missing mass distribution when the experimental smearing is included. Now the bump corresponding to the Higgs boson is below the $b\bar{b}$ background. The situation for some scenarios beyond the Standard Model may be better.

In Refs.[3, 4] we have discussed in great detail how to improve the difficult situation. Examples are shown in Fig.3. In the left panel we show the situation when a cut on differ-

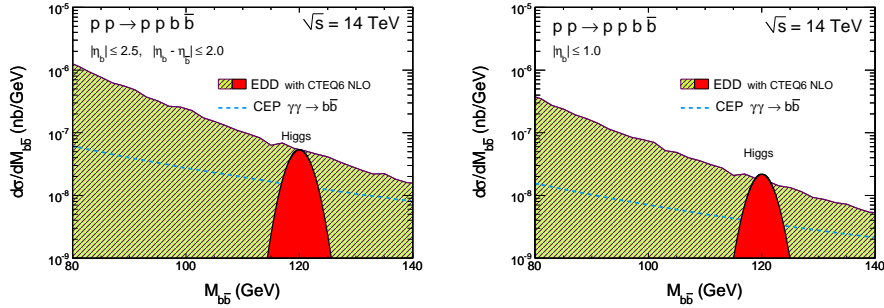


Figure 3: The $b\bar{b}$ invariant mass distribution for $\sqrt{s} = 14$ TeV. In the left panel the rapidity difference is limited to $(-1, 1)$ and in the right panel both pseudorapidities are restricted to $-1 < \eta < 1$.

ence of pseudorapidities is limited to the interval $(-1, 1)$ and in the right panel when cuts on pseudorapidity of b and \bar{b} are imposed. In both cases the situation seems much better than in the previous case. We have checked, however, that this is an optimal situation and further improvement of the signal-to-background ratio is in practice impossible.

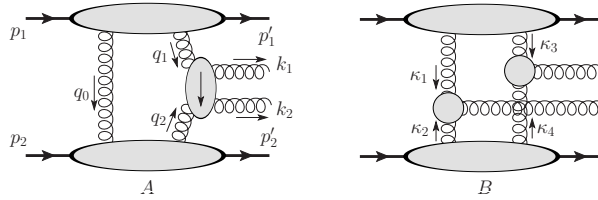


Figure 4: The mechanisms of the digluon production.

Now we come to the distributions for exclusive dijet production. The diagrams of the possible mechanisms are shown in Fig.4. The first diagram is the dominant mechanism of dijet production, whereas the second mechanism was discussed in more detail in our recent paper [5]. The details of the corresponding calculations can be found in [5]. In Fig.5 we show the total cross section as a function of minimal E_T . Already the digluon contribution (thick solid line) is slightly above the data. In the case of quark-antiquark dijets we present the contribution of $u\bar{u}$, $d\bar{d}$, $s\bar{s}$, $c\bar{c}$ and $b\bar{b}$. In the first three cases, we put

the quark masses to zero, and in the last two cases we take explicit masses known from the phenomenology (1.5 GeV and 4.75 GeV, respectively). The sum of all quark-antiquark contributions is shown in the right panel by the dash-dotted curve. We conclude that the quark-antiquark jet contribution is smaller by more than two orders of magnitude than the digluon one. However, the $b\bar{b}$ contribution can be essential e.g. as a background for Higgs searches in exclusive pp scattering.

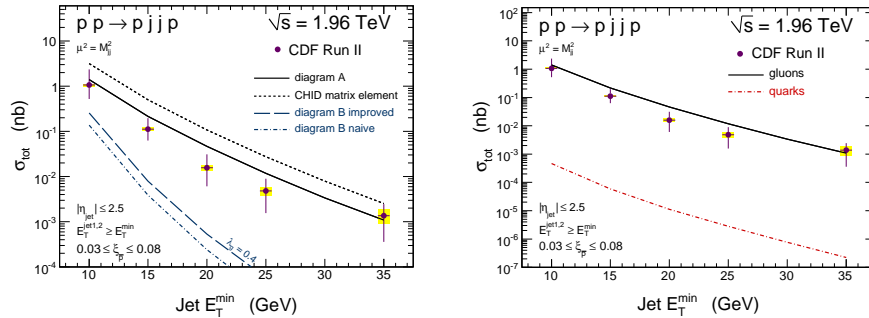


Figure 5: The total cross section for exclusive dijet production as a function of $E_{t,min}$. The experimental data points are taken from Ref. [13]. Left panel: digluon contribution for the standard mechanism with our matrix element (solid line) and CHID matrix element (short-dashed line), for diagram B (long-dashed line). Right panel: quark-antiquark (dash-dotted line) contribution.

The exceptional dominance of digluon jets over quark-antiquark jets found here offers an extraordinary condition for increased glueball production in gluon fragmentation [5]. In order to investigate it more one needs to study a contamination of central diffractive components where the proportions of digluonic to quark-antiquark are less favourable.

The gluonic jets can be misidentified as b -quark jets. For example the ATLAS misidentification factor is 1.4%. If both gluonic jets are misidentified then such a misidentified event can contribute to a background to exclusive Higgs boson production. In Fig.6 we illustrate the situation. We show both the Higgs signal (hatched area) including experimental resolution as well as diffractive $b\bar{b}$ continuum, QED $b\bar{b}$ continuum as well as formally reducible digluon contribution. In the calculation we have assumed that jet misidentification probability is 1.4%, i.e. we have multiplied the dijet cross section by a small number 0.014^2 . The obtained digluon contribution is even larger than the $b\bar{b}$ one

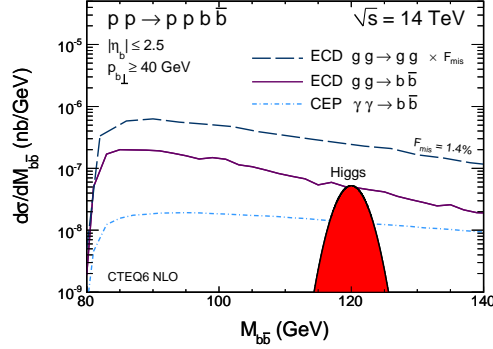


Figure 6: Invariant mass distribution of the $b\bar{b}$ system. Shown are contributions from diffractive Higgs boson (shaded area), $b\bar{b}$ continuum (solid line), $\gamma\gamma$ continuum (dash-dotted line) and diffractive digluon contribution (dashed line) multiplied by the ATLAS misidentification factor squared.

and overlays the Standard Model Higgs signal. In the case of Minimal Supersymmetric Model the situation can be more favourable. [11, 12].

4 Conclusions

We have shown and discussed differential distributions for the continuum $b\bar{b}$ production. Inclusion of the experimental resolution is necessary when comparing the Higgs signal and the $b\bar{b}$ background. Our analysis shows that a special cuts could be useful to see a signal above the continuum background. We have also shown a reducible background due to a misidentification of gluonic jets as b or \bar{b} jets.

Rough agreement of the theoretical dijet cross section with the Tevatron data gives more confidence to the predictions for exclusive Higgs boson production.

Our analysis indicates that a real experiment for the exclusive Higgs boson production can be rather difficult. The situation could be better for some scenarios beyond the Standard Model.

Acknowledgements

I am indebted to Rafał Maciuła and Roman Pasechnik for collaboration on the issues presented here.

References

- [1] V. A. Khoze, A. D. Martin and M. G. Ryskin, Phys. Lett. B **401**, 330 (1997);
A. B. Kaidalov, V. A. Khoze, A. D. Martin and M. G. Ryskin, Eur. Phys. J. C **33**,
261 (2004).
- [2] R. Maciuła, R. Pasechnik and A. Szczurek, Phys. Lett. B **685**, 165 (2010).
- [3] R. Maciuła, R. Pasechnik and A. Szczurek, arXiv:1006.3007 [hep-ph], Phys. Rev.
D82 114011 (2010).
- [4] R. Maciuła, R. Pasechnik and A. Szczurek, arXiv:1011.5842 [hep-ph]. Phys. Rev.
D83 114034 (2011).
- [5] R. Maciuła, R. Pasechnik and A. Szczurek, arXiv:1109.5517 [hep-ph].
- [6] R. S. Pasechnik, A. Szczurek and O. V. Teryaev, Phys. Rev. D **78**, 014007 (2008);
R. S. Pasechnik, A. Szczurek and O. V. Teryaev,
- [7] R. S. Pasechnik, O. V. Teryaev and A. Szczurek, Eur. Phys. J. C **47**, 429 (2006).
- [8] J. Pumplin et al., JHEP 0207, 012 (2002).
- [9] G. Passarino, Nucl. Phys. B **488**, 3 (1997).
- [10] A. Cisek, W. Schäfer and A. Szczurek, Phys. Rev. **D80** 074013 (2009).
- [11] B. E. Cox, F. K. Loebinger, A. D. Pilkington, JHEP **0710**, 090 (2007).
- [12] S. Heinemeyer, V.A. Khoze, M.G. Ryskin, W.J. Stirling, M. Tasevsky, and G. Weiglein, Eur. Phys. J. C **53** 231 (2008).
- [13] T. Aaltonen *et al.* [CDF Collaboration], Phys. Rev. D **77**, 052004 (2008);
A. A. Affolder *et al.* [CDF Collaboration], Phys. Rev. Lett. **88**, 151802 (2002);
A. A. Affolder *et al.* [CDF Collaboration], Phys. Rev. Lett. **85**, 4215 (2000).